

## Article

# Copper Extraction from Oxide Ore of Almalyk Mine by H<sub>2</sub>SO<sub>4</sub> in Simulated Heap Leaching: Effect of Particle Size and Acid Concentration

Chan-Ung Kang<sup>1</sup>, Seung-Eun Ji<sup>1</sup> , Thomas Pabst<sup>2</sup> , Kung-Won Choi<sup>1</sup> , Moonis Ali Khan<sup>3</sup> ,  
Rahul Kumar<sup>4</sup> , Prakash Krishnaiah<sup>1</sup> , Yosep Han<sup>5</sup> , Byong-Hun Jeon<sup>1,\*</sup>  and Do-Hyeon Kim<sup>1,\*</sup>

- <sup>1</sup> Department of Earth Resources and Environmental Engineering, Hanyang University, 222, Wangsimni-ro, Seongdong-gu, Seoul 04763, Korea; mr.ung1212@gmail.com (C.-U.K.); jsy8691@hanyang.ac.kr (S.-E.J.); kung@hanyang.ac.kr (K.-W.C.); ksp.shine@gmail.com (P.K.)
- <sup>2</sup> Département des Génies Civil, Géologique et des Mines (CGM), Polytechnique Montréal, Université d'ingénierie, Montréal, QC H3T 1J4, Canada; t.pabst@polymtl.ca
- <sup>3</sup> Chemistry Department, College of Science, King Saud University, Riyadh 11451, Saudi Arabia; moonisalikhan@gmail.com
- <sup>4</sup> Centre for Bio-Nanotechnology & Department of Chemistry (COBS & H), CCS Haryana Agricultural University, Hisar 125004, India; rahulkdhaka.iitr@gmail.com
- <sup>5</sup> Resources Recovery Research Center, Mineral Resources Division, Korea Institute of Geoscience and Mineral Resources (KIGAM), 124 Gwahak-ro, Yuseong-gu, Daejeon 34132, Korea; yosep@kigam.re.kr
- \* Correspondence: bhjeon@hanyang.ac.kr (B.-H.J.); kimdohyeon@hanyang.ac.kr (D.-H.K.)



**Citation:** Kang, C.-U.; Ji, S.-E.; Pabst, T.; Choi, K.-W.; Khan, M.A.; Kumar, R.; Krishnaiah, P.; Han, Y.; Jeon, B.-H.; Kim, D.-H. Copper Extraction from Oxide Ore of Almalyk Mine by H<sub>2</sub>SO<sub>4</sub> in Simulated Heap Leaching: Effect of Particle Size and Acid Concentration. *Minerals* **2021**, *11*, 1020. <https://doi.org/10.3390/min11091020>

Academic Editors: Weiguo Xie, Hylke J. Glass and Eiman Amini

Received: 25 August 2021

Accepted: 15 September 2021

Published: 18 September 2021

**Publisher's Note:** MDPI stays neutral with regard to jurisdictional claims in published maps and institutional affiliations.



**Copyright:** © 2021 by the authors. Licensee MDPI, Basel, Switzerland. This article is an open access article distributed under the terms and conditions of the Creative Commons Attribution (CC BY) license (<https://creativecommons.org/licenses/by/4.0/>).

**Abstract:** In this investigation, a laboratory-scale study to extract copper (Cu) from its oxide ore (0.425–11.2 mm particle size) was conducted using varied sulfuric acid (H<sub>2</sub>SO<sub>4</sub>) concentrations (0.05–0.5 M) as a lixiviant. Through a physicochemical and mineralogical analysis of real field ore samples from the Almalyk mine heap site (Tashkent, Uzbekistan), malachite was identified as a Cu-bearing mineral. Extraction rates were analyzed according to the ore particle size and acid concentration. The Cu extraction with the smallest particle size (in 24 h) varied between 76.7% and 94.26% at varied H<sub>2</sub>SO<sub>4</sub> concentrations (0.05–0.5 M). Almost half (50%) of Cu was extracted from the ore within 4 and 72 h of contact time for 0.425–2 mm and 5.6–11.2 mm particle sizes, respectively, using 0.15 M H<sub>2</sub>SO<sub>4</sub>. Weeklong leaching experiments with 0.5 M H<sub>2</sub>SO<sub>4</sub> revealed a higher copper extraction rate (≥73%) from coarse ore particles (5.6–11.2 mm). Along with the copper extraction, iron (29.6 wt%), aluminum (70.2 wt%), magnesium (85.4 wt%), and calcium (44.4 wt%) were also leached out considerably through the dissolution of silicate and carbonate gangue minerals. In this study, an 80.0–94.26% copper extraction rate with reduced acid consumption (20%) proved to be a cost-effective approach.

**Keywords:** heap leaching; copper extraction; copper oxide; malachite; acid consumption

## 1. Introduction

Copper (Cu) is a widely used metal that is applied in electrical, electronics, construction, and manufacturing sectors [1,2]. Currently, two important extraction methods are employed: pyrometallurgy and hydrometallurgy. Pyrometallurgy is a conventional method (concentration–smelting–refining) generally used to extract Cu from its ores [3]. However, pyrometallurgy has been used mainly for sulfide flotation concentrates instead of its ores and is economically achievable with industrial-scale production, but only if the feeding material is a Cu-rich ore [4]. By contrast, hydrometallurgy is an important Cu extraction method used extensively worldwide. Different oxides of Cu such as tenorite (CuO), malachite (Cu<sub>2</sub>(OH)<sub>2</sub>CO<sub>3</sub>), and chrysocolla ((Cu,Al)<sub>2</sub>H<sub>2</sub>Si<sub>2</sub>O<sub>5</sub>(OH)<sub>4</sub>·nH<sub>2</sub>O) are easily dissolved with a cost-effective acid lixiviant such as sulfuric acid (H<sub>2</sub>SO<sub>4</sub>) [5–7]. Therefore, hydrometallurgical processes, including leaching, solvent extraction, and electro-winning,

are considered as favorable and cost-effective approaches for copper extraction from oxide ores [8,9].

Leaching is the first step of the hydrometallurgical process of Cu extraction, which includes the dissolution of Cu from its raw ore into an aqueous phase. In most of the cases, excavated ores are stacked near the mine site and dilute  $H_2SO_4$  is poured from the top of the reactor. The movement of leachate along with  $H_2SO_4$  through a fixed bed of ore particles enables the target metal to be leached into the aqueous phase, and the same is collected downward through gravity [10]. This type of leaching is called “heap leaching”. There are other methods that are similar to heap leaching, such as dump, in situ, and vat leaching, which differ slightly from each other in terms of the methodology and ore grade [11].

The method of heap leaching has been widely used to extract copper because of its low operational cost, proximity to the site, simplicity in operation, short time for construction, good yield, and environmental advantages [12,13]. As high-grade copper ores are depleting globally, this approach is economical and facile and has, hence, received considerable attention among copper extraction experts. Among different applications of heap leaching, copper extraction from its oxide ores has been relatively less explored for a long time, except for a few reports [14,15].

Using an appropriate identification technique for leaching behavior is important during Cu extraction from its ore. Previous reports suggest that the kinetics of leaching experiments using  $H_2SO_4$  only lasted for a short time (few minutes to several hours) and only on fine-grained ores (ten to hundreds of micrometers). A few research groups [6,16] investigated the dissolution kinetics of malachite, whereas others conducted studies on chrysocolla leaching with dilute  $H_2SO_4$  [17,18]. Leaching kinetics of various Cu oxide ores such as tenorite [1], cuprite ( $Cu_2O$ ) [19], and atacamite ( $Cu_2Cl(OH)_3$ ) [20] have been examined. To the best of the authors’ knowledge, the Cu leaching kinetics have been thoroughly explained based on the shrinking core model or logarithmic function. Some long-term industrial-scale extractions of Cu were performed taking coarse grains of ores (millimeter to centimeter size) [3,10]. However, a few limitations exist in applying the previous outcome for Cu leaching, especially on an industrial scale. Detailed studies explaining accompanied processes such as the dissolution of gangue minerals and changes in the ionic properties of leachate in the ore leaching process are required. There is also a study that Cu is adsorbed on the surface of gangue minerals such as smectites and mordenite with high CEC (Cation Exchange Capacity), reducing the amount of extraction [21].

The present study investigated the leaching behavior of Cu from its oxide ore throughout a weeklong (7 days) experiment using different sizes of ore particles, mimicking the heap environment. A series of experiments were conducted to check the dissolution of metals during the leaching process. Throughout the experiments, different concentrations of  $H_2SO_4$  were employed to examine the effect of acidity on Cu leaching. This study also investigated the economic perspectives and the amount of acid consumption during leaching experiments. A sufficient leaching efficiency on larger particle ores and lower concentration of acids led to reduced crushing costs and chemical consumption, respectively.

## 2. Materials and Methods

### 2.1. Sample Collection Site

The CuO ore samples were collected from Almalyk mine, the largest non-ferrous open-pit mine located in the Western Central Asian Orogenic Belt, near Tashkent, Uzbekistan (Figure 1). The Almalyk copper mine has contained tons of copper in mineral oxide form since the early 1960s [22]. This Cu is of the porphyry type and covers approximately 50–75% of global Cu production. Gold, silver, zinc, and lead were also produced from these mines [23,24]. The Almalyk porphyry group comprises different deposits, namely Kalmakyr, Sarycheku, and Dalnee. The samples used in this study were collected from the mine site close to the Kalmakyr deposit. Kalmakyr (discovered in 1947) is the largest Cu–Au porphyry deposit in the Almalyk region, with 3700 million tons of measured and

indicated Cu resources [22,25]. Geologically, the mineralization of major ore bodies consisting of oxidized, leached, and secondary sulfide-enriched zones range from the surface to 60 m deep [26]. The principal mineral within the oxidized zone is malachite, with chrysocolla being locally important [22]. In the primary sulfide-enriched zone, chalcopyrite and bornite ( $\text{Cu}_5\text{FeS}_4$ ) exist as major copper minerals. The gangue minerals comprise quartz ( $\text{SiO}_2$ ), feldspar ( $(\text{K}, \text{Na}, \text{Ca})\text{AlSi}_3\text{O}_8$ ), biotite ( $\text{K}(\text{Mg}, \text{Fe})_3(\text{AlSi}_3\text{O}_{10})(\text{OH})_2$ ), chlorite ( $(\text{Mg}, \text{Fe})_3(\text{Si}, \text{Al})_4\text{O}_{10}(\text{OH})_2 \cdot (\text{Mg}, \text{Fe})_3(\text{OH})_6$ ), sericite ( $\text{KAl}_2(\text{AlSi}_3)_{10}(\text{OH})_2$ ), anhydrite ( $\text{CaSO}_4$ ), and calcite ( $\text{CaCO}_3$ ) [26]. A substantial amount of Cu has been extracted from chalcopyrite and bornite (copper sulfide ores) at the open-pit mine site of Kalmakyr. However, a significant quantity of ores remains excavated from the oxidized zone and is stockpiled near the mine site. The ores may be used for Cu extraction via heap leaching using  $\text{H}_2\text{SO}_4$ .



**Figure 1.** Location of the oxide heap in Almalıy mine, Uzbekistan.

## 2.2. Sample Preparation and Characterization

Physicochemical properties of raw ore samples were examined to confirm the presence of Cu-bearing and gangue minerals. The ore samples were crushed to less than 1 cm using a jaw crusher. The aqua regia ( $\text{HCl}:\text{HNO}_3$ , 3:1 *v/v*) method (ISO 11466) was used to digest the samples. An inductively coupled plasma-optical emission spectrometer (ICP-OES; VARIAN, 720-ES, Palo Alto, Santa Clara, CA, USA) was used to investigate the composition of the extractable metals of the ores (particle size of  $<150\ \mu\text{m}$ ).

The mineral content of the ores was estimated through X-ray diffraction (XRD; Rigaku, SmartLab, Tokyo, Japan), reflecting microscopy (Leica, DVM2500 VZ80, Wetzlar, Germany), polarization microscopy (Leica, DM750P, Wetzlar, Germany), and scanning electron microscopy coupled with energy dispersive X-ray spectrometry (SEM-EDS; FEI, Verios G4 UC, Hillsboro, OR, USA). For reflecting microscopy and SEM-EDS, the ore samples were polished with sandpaper to ensure a smooth surface. A thin section was prepared to observe the minerals present in the ore under the polarization microscope.

### 2.3. Leaching Experiments

To determine the effect of particle size on Cu leaching, different sizes of the ore samples (0.425–2, 2–5.6, and 5.6–11.2 mm) were prepared. The effect of H<sub>2</sub>SO<sub>4</sub> concentration (0.05–0.5 M) on the dissolution of Cu and other metal ions in ore samples was checked. An aliquot of H<sub>2</sub>SO<sub>4</sub> (500 mL) was agitated with an ore sample (100 g) for a week (7 days) using an incubator shaker (25 °C, 150 rpm). Malachite, a carbonate form of copper, upon reacting with H<sub>2</sub>SO<sub>4</sub> produces carbon dioxide (CO<sub>2</sub>); hence, the reactor bottle was covered with a perforated paper foil to avoid gas pressure. The pH of the suspension was periodically checked using a fixed amount of collected aliquot (3 mL). The pH of the suspension was adjusted to initial pH by adding a 5 M H<sub>2</sub>SO<sub>4</sub> solution when more than 50% of the initial acid was consumed. A sampled pregnant leaching solution (PLS) was filtered (0.45 µm) and followed by Cu, Fe, Al, Mg, and Ca analysis using ICP-OES. After a weeklong (7 days) leaching experiment, the total dissolved solids (TDS) were measured for each PLS. The ores, after the reaction, were washed with deionized (DI) water and dried at 80 °C for 24 h to conduct XRD analysis.

## 3. Results and Discussion

### 3.1. Characterization of the Ore Samples

The elemental compositions of the ore samples are shown in Table 1. The average Cu contents of the sample, determined via an ICP-OES analysis (1.56 wt%), are valuable, as the general Cu grade (in porphyry deposits) is in the range between 0.3 and 2.5 wt% [27]. The extracted Cu (0.35 wt%) exceeded its original content (0.28 wt%), which might have been caused by the heterogeneity of ore samples. The residual elements were not released during digestion, as they are considered as bound to silicate minerals [28], and may require more time for extraction. The XRD analysis (Figure 2a) indicated that malachite was the main Cu-bearing mineral in the ore, whereas gangue minerals contained quartz, orthoclase, muscovite, and chlorite. Several ore samples also contained albite and biotite as gangue minerals. Malachite was the most important Cu oxide mineral, as it contained 57.5% Cu stoichiometrically [7,16]. The gangue minerals were the same as silicate minerals, which were commonly present in porphyry Cu deposits and the Kalmakyr deposit, Uzbekistan [29].

**Table 1.** Composition of element eluted through aqua regia extraction in the ore sample collected from Almalyk mine in Uzbekistan.

| Elements | ICP-OES (%) * |
|----------|---------------|
| Cu       | 1.56          |
| Fe       | 4.10          |
| Al       | 0.588         |
| Mg       | 0.422         |
| Ca       | 0.345         |

\* Ore sample was digested in aqua regia (ISO 11466).

The dominant minerals in the ore and their microstructure were studied using SEM-EDS and optical microscopy, respectively. The greenish color of the malachite minerals (Figure 3) was observed using both the reflecting and polarization microscopes. The texture of the greenish mineral in the polarization microscope image showed a fibrous or needle-like shape (Figure 3a,b), which is a general crystal habit of malachite [30]. The micro-scale visualization of the greenish mineral specimen by SEM is shown in Figure 3d. The elemental analysis detected peaks of Cu, C, and O, thereby proving the presence of malachite (Figure 3e). Quartz, feldspars, and iron-rich chlorite and biotite were also examined by optical microscopes and SEM-EDS.

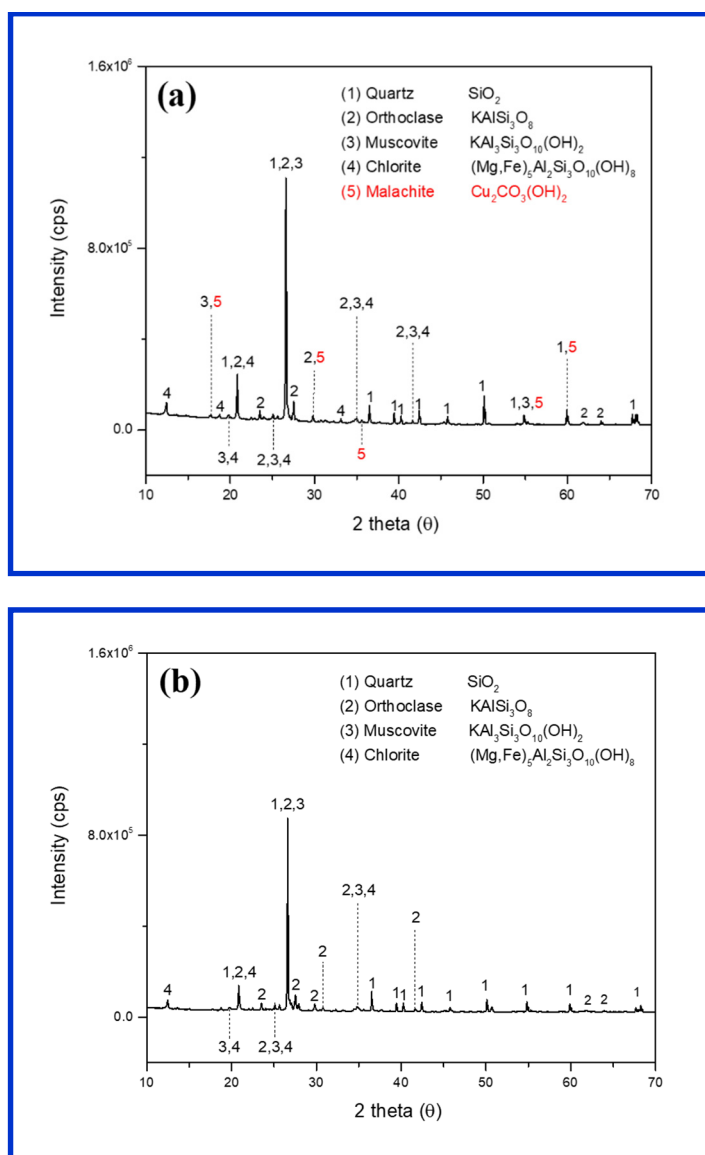


**Figure 2.** X-ray diffraction studies of ore samples before leaching (a) and after a weeklong (7 days) leaching with  $\text{H}_2\text{SO}_4$  (0.15 M) (b).

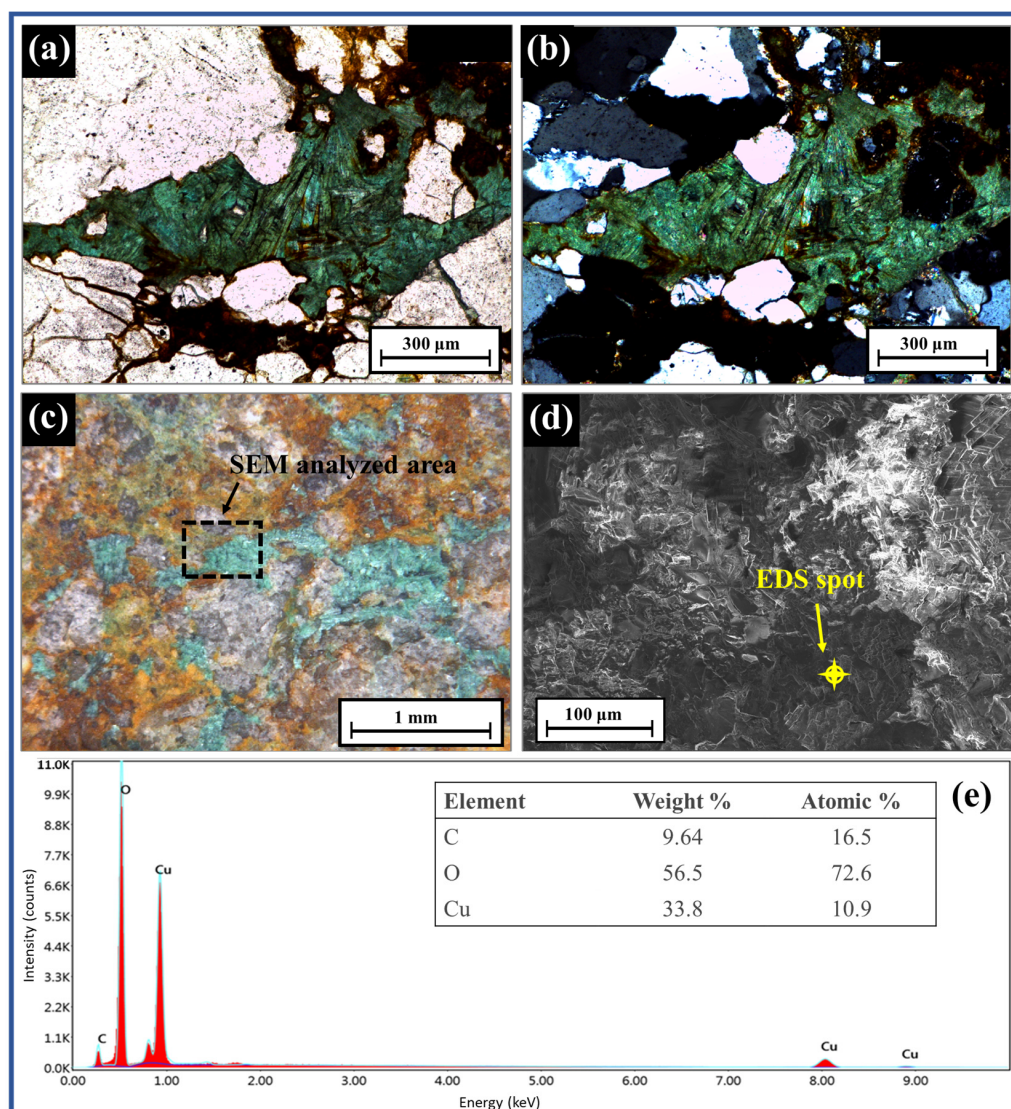
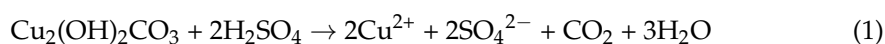


**Figure 3.** Polarization microscope images with open Nicol (a) and crossed Nicol (b); reflection microscope image (c), SEM image (d), and elemental analysis (%) of ore (e).

### 3.2. Leaching Experiments

#### 3.2.1. Dissolution of Malachite

The reaction of malachite dissolution with  $\text{H}_2\text{SO}_4$ , which occurred in a reactor during the batch leaching, was as follows:



Herein, Cu released into the solution by consuming the protons from  $\text{H}_2\text{SO}_4$ . During the leaching experiments, the solution color changed from transparent to blue (Figure 4), indicating the dissolution of divalent copper ions.

A change during the weeklong (7 days) reaction with 0.15 M  $\text{H}_2\text{SO}_4$  was visually observed (Figure 5). The green color of malachite both inside and outside the ores disappeared and turned into white after leaching. The XRD analysis of the same ores also confirmed the disappearance of malachite and the presence of only gangue minerals (Figure 2b). Thermodynamically, the dissolution of malachite in acidic sulfate solution started at pH 4, and gradually completed below pH 3 [16]. The weakest acidic condition (0.05 M  $\text{H}_2\text{SO}_4$ ) during this experiment showed an average pH of 1.45. Thus, the malachite that could

contact protons was completely dissolved during the mass transport between the  $\text{H}_2\text{SO}_4$  solution and mineral surface.

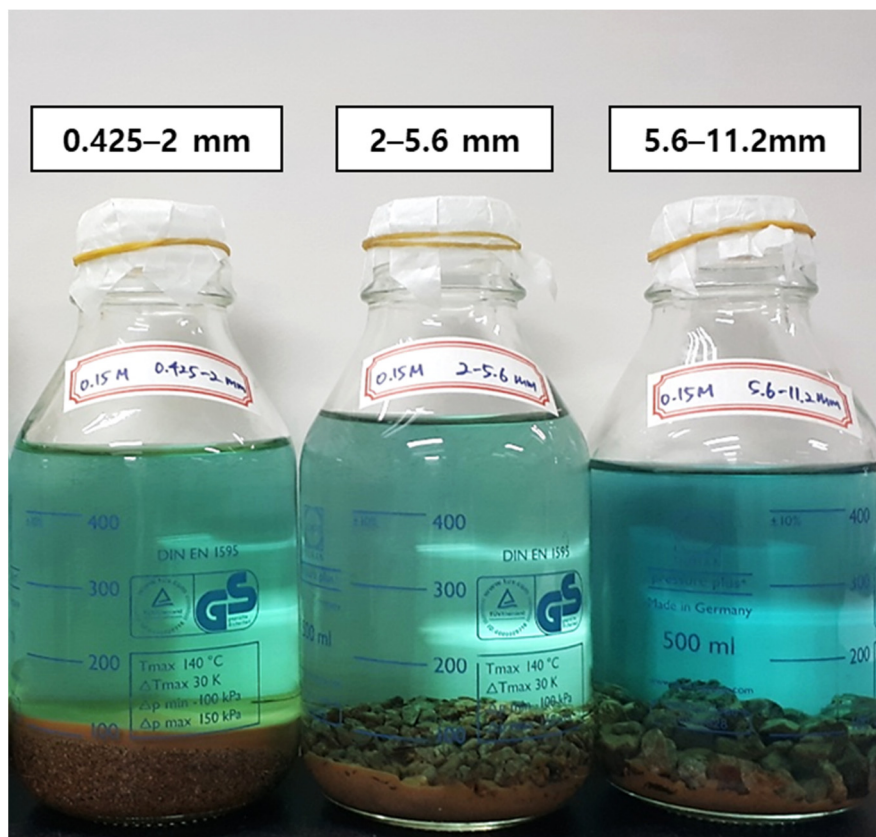


Figure 4. Pregnant leaching solution after weeklong (7 days) reaction.

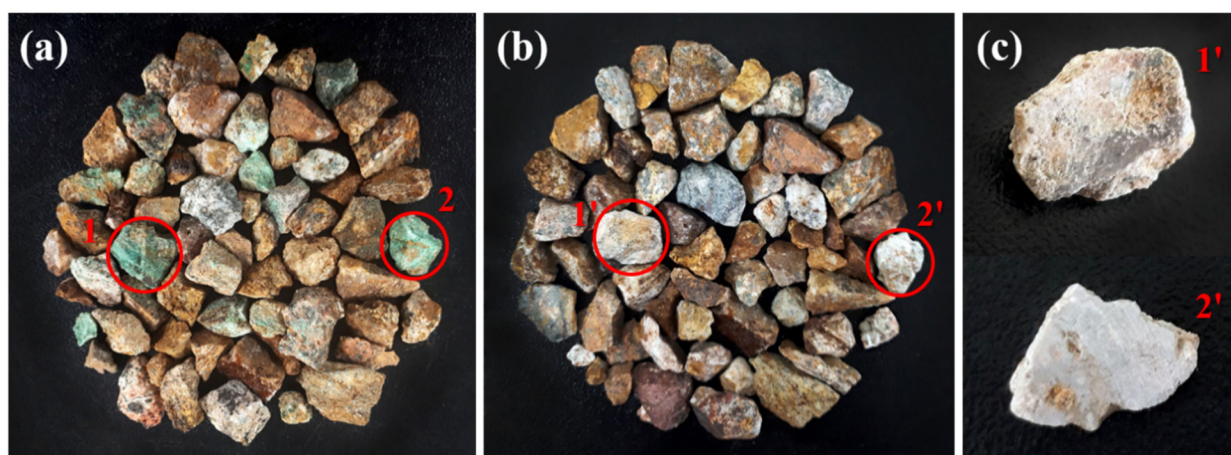
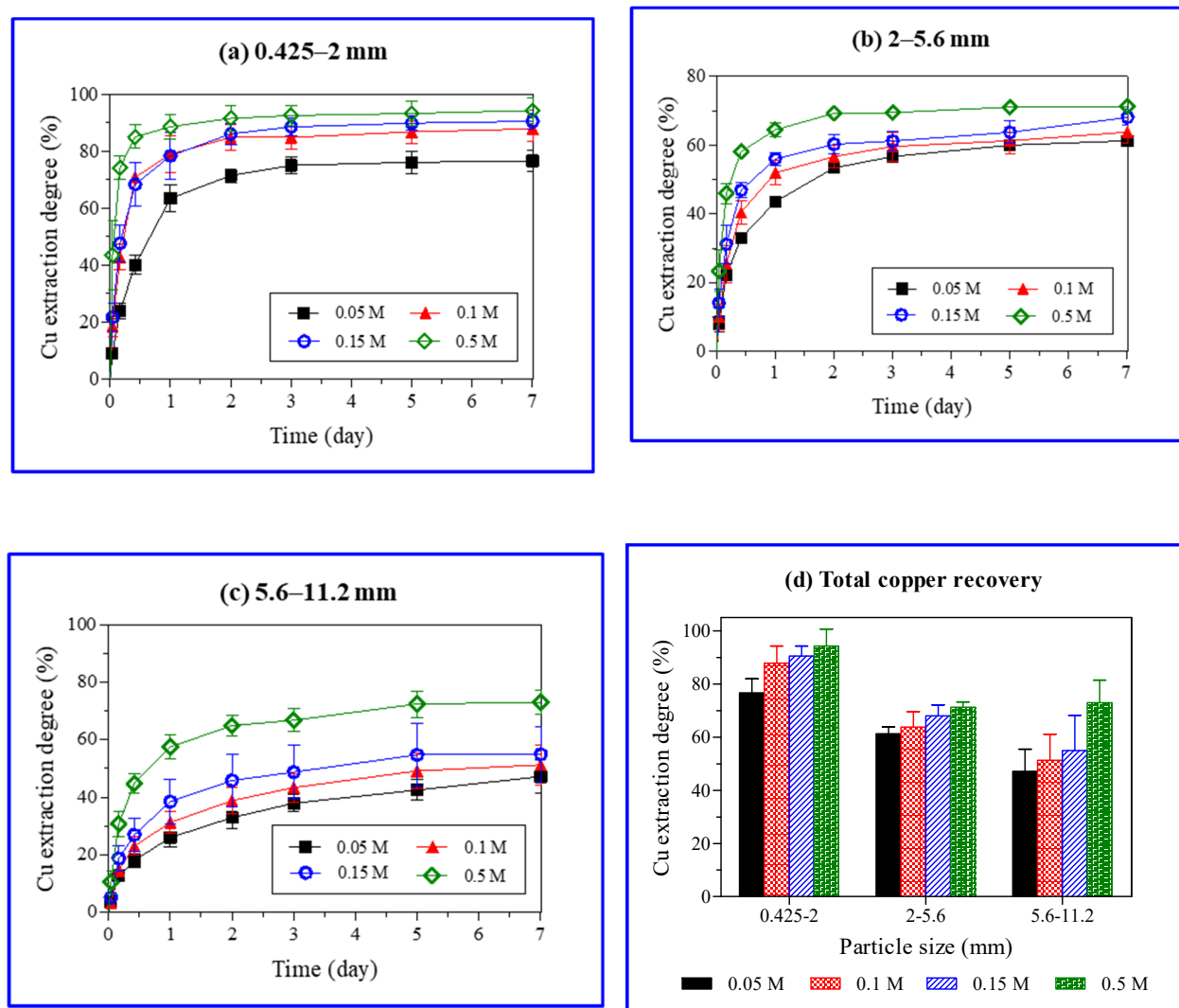


Figure 5. Photographs of raw ore (a), sulfuric acid ( $\text{H}_2\text{SO}_4$ , 0.15 M)-treated ore (b) (after a weeklong, 7 days experiment), and cross-section of leached ore (c) (1, 2: ore containing malachite before reaction; 1', 2': ore after malachite leaching reaction).

### 3.2.2. Effect of Ore Particle Size and Sulfuric Acid Concentration on Copper Extraction

The results of Cu extraction from ore during the weeklong (7 days) batch experiments with varied ore particle size and  $\text{H}_2\text{SO}_4$  concentration are shown in Figure 6. In this study, 7 days leaching was sufficient to reach equilibrium and longer leaching was deemed non necessary. The maximum amount of Cu was extracted from the smallest (0.425–2 mm)

particles of ore and the highest  $\text{H}_2\text{SO}_4$  concentration (0.5 M). The Cu extraction was determined by dividing the copper concentration in PLS with an average copper grade (1.56 wt%). The Cu extraction with the smallest particle size (0.425–2 mm) varied from 11.4 to 88.6% with increasing  $\text{H}_2\text{SO}_4$  concentrations (0.05–0.5 M) in 24 h.



**Figure 6.** Effect of particle size and sulfuric acid ( $\text{H}_2\text{SO}_4$ ) concentration on copper extraction degree (%) with time (a–c) and total copper recoveries (%) after a weeklong (7 days) experiment (d).

Approximately half (50%) of the Cu was extracted with 0.15 M  $\text{H}_2\text{SO}_4$  after 4 and 72 h from the ore particles with sizes of 0.425–2 and 5.6–11.2 mm, respectively. The large surface area of fine particles (0.425–2 mm) promoted a rapid reaction between the malachite and protons, leading to a rapid Cu dissolution in the ore. An increase in the ore particle size resulted in a decrease in Cu extraction (Figure 6). The strong acidity (0.5 M  $\text{H}_2\text{SO}_4$ ) overshadowed the effect of the ore particle size, showing a higher Cu extraction, especially from the ore of the largest particle size (5.6–11.2 mm).

### 3.2.3. Leaching Kinetics of Copper from Ore

The Cu leaching was initially rapid, gradually slowed, and, finally, stabilized when Cu extraction was arrested. The overall Cu leaching can be interpreted by a shrinking core model, which includes a surface chemical reaction and proton diffusion through the product layer. The shrinking core model represents heterogeneous reactions between the fluid ( $\text{H}_2\text{SO}_4$ ) and solid surface (ore particles) [31]. As widely accepted, to explain the leaching

kinetics of Cu oxide ores in most of the studies [1,16–19,32,33], the shrinking core model may well describe the Cu leaching kinetics followed in the present investigation. Based on the dissolution behavior of Cu and other metals, the leaching behavior of Cu can be divided into three steps: (i) extremely rapid leaching of Cu owing to the dissolution of free malachite on the ore surface, (ii) a gradual decrease in the Cu dissolution rate, and (iii) the decomposition of high to moderate soluble silicate gangue minerals and the reaction of the malachite wrapped inside them with the acid. The third step corresponds to the part, which is the almost horizontal slope of the graph, as shown in Figure 6. Moderately to poorly soluble silicate minerals dissolved continuously, and the Cu minerals trapped inside dissolved. A similar interpretation involving three-step dissolution kinetics has been proposed elsewhere [32].

The ore particle size significantly influenced the rate by three-step leaching reactions. Acid and minerals, initially contacted superficially followed by the entry of acid into the ore via small pores leading to continuous chemical reactions and mineral dissolution. The ore grain size was a critical factor as the mass transfer process enabled the leaching of metals in ore and influenced the leaching kinetics. The large ore particle size (i.e., small specific surface area) could lead to a slow reaction at the internal pores. Thus, once the minerals near the surface pores dissolved, they created deep micro-pores resulting in steady and slow leaching.

The data of dissolved ions and TDS in PLS during a weeklong (7 days) leaching experiment are provided in Table 2. The concentration of metals increased in the case of fine ore particles and with a high acid concentration (0.5 M H<sub>2</sub>SO<sub>4</sub>). The sulfate ions (SO<sub>4</sub><sup>2−</sup>) in PLS contributed to TDS because of the addition of H<sub>2</sub>SO<sub>4</sub> into the solution. An increase in the acidity and specific surface area caused metal dissolution from gangue minerals. Potassium and silicon in gangue minerals (Figure 2), other than the metals under investigation, may have also contributed to TDS. The difference between TDS and SO<sub>4</sub><sup>2−</sup> increased (7.47 to 25.79 g/L) with a rise in the H<sub>2</sub>SO<sub>4</sub> concentration (0.05 to 0.5 M; 0.425–2 mm) and decreased (10.31 to 7.2 g/L) with the ore particle size (0.425–2 to 5.6–11.2 mm; 0.15 M H<sub>2</sub>SO<sub>4</sub>).

**Table 2.** Metals (Cu, Fe, Al, Ca, Mg), sulfate, and total dissolved solids (TDS) in a pregnant leaching solution (PLS) of ore after a weeklong (7 days) leaching experiment.

| Particle Size (mm) | Concentration of H <sub>2</sub> SO <sub>4</sub> (M) | Cu (g/L) | Fe (g/L) | Al (g/L) | Ca (g/L) | Mg (g/L) | SO <sub>4</sub> <sup>2−</sup> (g/L) * | TDS (g/L) | Cu Yield (wt%) |
|--------------------|---|----------|----------|----------|----------|----------|---------------------------------------|-----------|----------------|
| 0.425–2            | 0.05  | 2.64     | 0.498    | 0.359    | 0.498    | 0.235    | 10.8                                  | 18.3      | 76.6           |
|                    | 0.10  | 2.74     | 1.05     | 0.449    | 0.490    | 0.330    | 17.2                                  | 27.2      | 87.9           |
|                    | 0.15  | 2.83     | 1.31     | 0.575    | 0.507    | 0.440    | 19.9                                  | 30.2      | 90.6           |
|                    | 0.50  | 2.94     | 3.63     | 1.20     | 0.474    | 1.10     | 69.0                                  | 94.8      | 94.3           |
| 2–5.6              | 0.05  | 1.91     | 0.378    | 0.260    | 0.426    | 0.189    | 10.6                                  | 17.4      | 61.3           |
|                    | 0.10  | 1.99     | 0.713    | 0.399    | 0.405    | 0.320    | 15.2                                  | 24.6      | 63.8           |
|                    | 0.15  | 2.12     | 1.15     | 0.563    | 0.469    | 0.471    | 23.5                                  | 33.1      | 68.1           |
|                    | 0.50  | 2.22     | 2.92     | 1.08     | 0.446    | 0.984    | 65.2                                  | 85.5      | 71.3           |
| 5.6–11.2           | 0.05  | 1.47     | 0.224    | 0.197    | 0.299    | 0.114    | 8.3                                   | 14.9      | 47.2           |
|                    | 0.10  | 1.60     | 0.647    | 0.398    | 0.340    | 0.260    | 15.5                                  | 22.7      | 51.3           |
|                    | 0.15  | 1.72     | 0.925    | 0.442    | 0.316    | 0.318    | 23.6                                  | 30.8      | 55.0           |
|                    | 0.50  | 2.28     | 2.43     | 0.829    | 0.311    | 0.717    | 64.3                                  | 84.2      | 73.0           |

\* Calculated from the amount of H<sub>2</sub>SO<sub>4</sub> added to the solution (the pH of the suspension was adjusted to initial pH by adding 5 M H<sub>2</sub>SO<sub>4</sub> solution when more than 50% of the initial acid was consumed).

### 3.2.4. Dissolution of Metal Ions from Gangue Minerals

Iron, aluminum, manganese, and calcium were analyzed after the reaction with acid (H<sub>2</sub>SO<sub>4</sub>) (Table 2). The acid (H<sub>2</sub>SO<sub>4</sub>) treatment caused the leaching of iron, aluminum, manganese, and calcium from gangue minerals in the ores. The XRD analysis did not reveal that these atoms were eluted from gangue minerals, as it was not able to identify all minerals containing those atoms (Figure 2). Dissolved ions showed, however, that other

minerals such as calcite and biotite were also dissolved through various chemical reactions (Table 3) [34–36]. Figure 7 presents the leaching kinetics of metal from ores with particle sizes in the range of 5.6–11.2 mm and various H<sub>2</sub>SO<sub>4</sub> concentrations (0.05, 0.1, 0.15, and 0.5 M). The dissolution (%) of copper along with iron, aluminum, magnesium, and calcium increased over the reaction time.

**Table 3.** Acid dissolution of typical gangue minerals.

| Solubility         | Mineral    | Chemical Reaction  |
|--------------------|------------|--|
| Readily Soluble    | Calcite    | $\text{CaCO}_3 + 2\text{H}^+ = \text{Ca}^{2+} + \text{H}_2\text{CO}_3$   |
|                    | Biotite    | $\text{K}(\text{Fe, Mg})_3\text{AlSi}_3\text{O}_{10}(\text{OH})_2 + 10\text{H}^+ = \text{K}^+ + 2(\text{Fe, Mg})^{2+} + \text{Al}^{3+} + 3\text{H}_4\text{SiO}_4$            |
| Moderately Soluble | Chlorite   | $(\text{Fe, Mg})_5\text{Al}_2\text{Si}_3\text{O}_{10}(\text{OH})_8 + 16\text{H}^+ = 5(\text{Mg, Fe})^{3+} + 2\text{Al}^{3+} + 3\text{H}_4\text{SiO}_4 + 6\text{H}_2\text{O}$ |
|                    | Pyroxene   | $\text{Ca}(\text{Mg, Fe})\text{Si}_2\text{O}_6 + 4\text{H}^+ + 2\text{H}_2\text{O} = \text{Ca}^{2+} + (\text{Mg, Fe})^{3+} + 2\text{H}_4\text{SiO}_4$                        |
|                    | Anorthite  | $\text{CaAl}_2\text{Si}_2\text{O}_8 + 8\text{H}^+ = \text{Ca}^{2+} + 2\text{Al}^{3+} + 2\text{H}_4\text{SiO}_4$  |
| Poorly Soluble     | Muscovite  | $\text{KAl}_3\text{Si}_3\text{O}_{10}(\text{OH})_2 + 10\text{H}^+ = \text{K}^+ + 3\text{Al}^{3+} + 3\text{H}_4\text{SiO}_4$  |
|                    | Albite     | $\text{NaAlSi}_3\text{O}_8 + 4\text{H}^+ + 4\text{H}_2\text{O} = \text{Na}^+ + \text{Al}^{3+} + 3\text{H}_4\text{SiO}_4$   |
|                    | Orthoclase | $\text{KAlSi}_3\text{O}_8 + 4\text{H}^+ + 4\text{H}_2\text{O} = \text{K}^+ + \text{Al}^{3+} + 3\text{H}_4\text{SiO}_4$   |
|                    | Quartz     | $\text{SiO}_2 + 2\text{H}_2\text{O} = \text{H}_4\text{SiO}_4$  |
|                    | Anhydrite  | $\text{CaSO}_4 = \text{Ca}^{2+} + \text{SO}_4^{2-}$  |

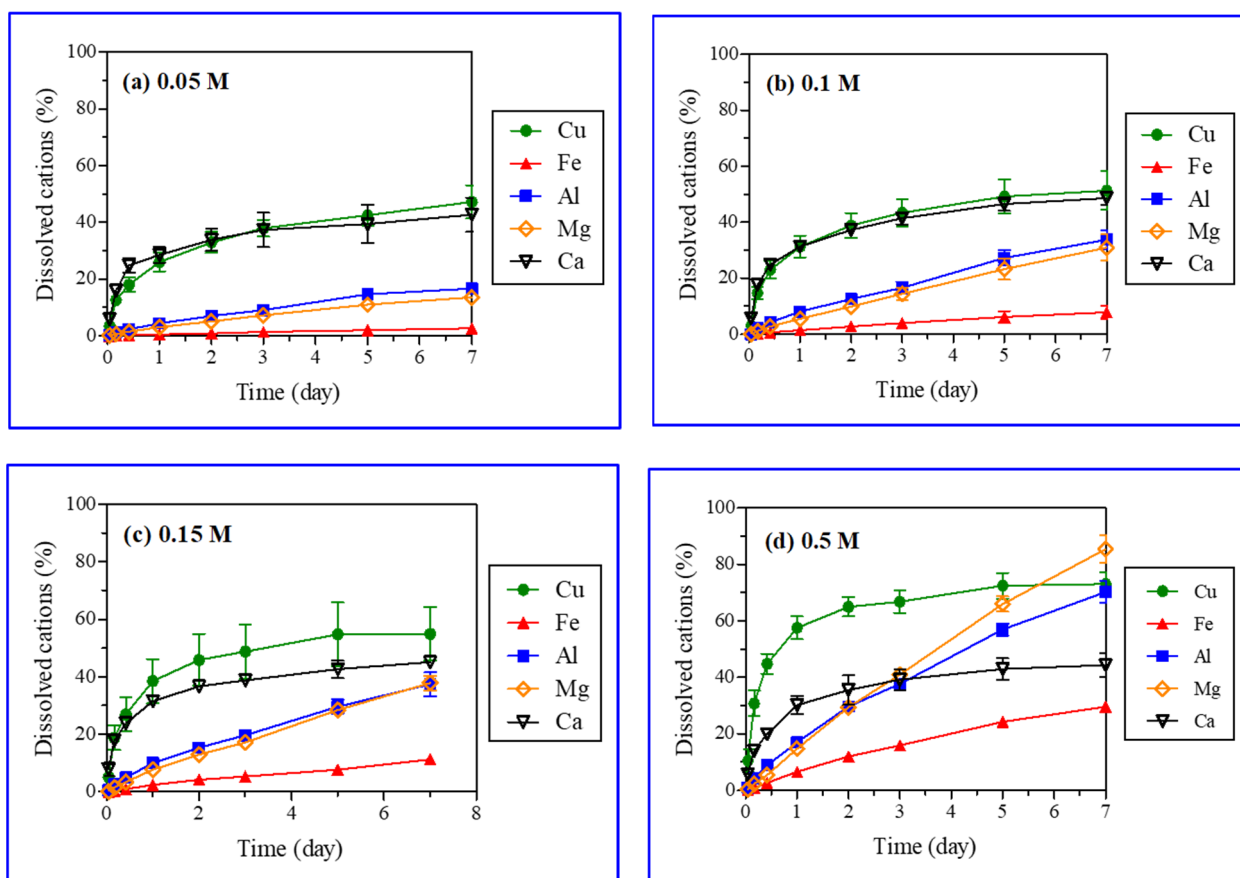


**Figure 7.** Leaching kinetics of metals with selected ore particle size (5.6–11.2 mm) and sulfuric acid (H<sub>2</sub>SO<sub>4</sub>) concentrations (0.05 M (a), 0.1 M (b), 0.15 M (c), and 0.5 M (d)).

Linear and logarithmic leaching patterns of metal ions with time and the acid concentration were observed in Figures 6 and 7, respectively. The concentrations of aluminum, magnesium, and iron in PLS increased linearly with time. Further, the leaching of metal ions increased substantially (Fe: 2.7 to 29.6 wt%, Al: 16.7 to 70.2 wt%, Mn: 13.6 to 85.4 wt%)

with a rise in the  $\text{H}_2\text{SO}_4$  concentration (0.05 to 0.5 M). However, the effect of  $\text{H}_2\text{SO}_4$  concentration on calcium leaching was negligible (42.7 and 48.6% from Figure 7). Calcium and copper showed similar leaching behaviors (logarithmic pattern); the leaching initially increased rapidly followed by a gradual decrease with time as reported in the literature for the  $\text{H}_2\text{SO}_4$  dissolution of malachite [6]. The fast early stage leaching of calcium might be attributed to calcite ( $\text{CaCO}_3$ ) dissolution. Calcite dissolves readily in acids, being the most aggressive acid consumer [37,38]. The leaching patterns of metals other than copper were different, as their leaching rates increased linearly with time (Figure 7). Calcite and malachite reacted quickly with acids and completely dissolved, resulting in the simultaneous leaching of calcium and copper, respectively. A similar leaching of calcium (40–50%) at varied  $\text{H}_2\text{SO}_4$  concentrations (0.05–0.5 M) implied that calcite was a major mineral form of calcium present in the ores. The remaining portion of calcium (50–60%), which existed as anhydrite ( $\text{CaSO}_4$ ) or anorthite ( $\text{CaAl}_2\text{Si}_2\text{O}_8$ ), had a poor and moderate acid solubility, respectively. Although calcite, anhydrite, and anorthite were not detected in the XRD analysis of ore samples, these minerals were, nonetheless, included in the major gangue minerals present at the Kalmakyr ore deposit [26].

The dissolution patterns of silicate minerals with more complex kinetics are different from those of carbonate minerals [38]. A linear increase in iron, magnesium, and aluminum concentrations in leachate over time was caused by the dissolution of silicate gangue minerals in the ore (Figure 7). Biotite and chlorite, displaying high and medium acid solubility, respectively, may have significantly contributed iron, magnesium, and aluminum. Muscovite, albite, orthoclase, and quartz were not dissolved in the acid and, thus, did not contribute to the generation of metal ions.

In the reactions of silicate minerals with protons, their structures can completely or partially collapse, leading to the release of metal ions [39] forming silica gel (owing to the polymerization of silica in the solution) and silica residue, respectively. An increase in the amount of amorphous silica can be a factor responsible for low copper extraction because of precipitation on the ore surface and a decrease in permeability [40,41]. The intensities of peaks in the XRD spectrum of acid-treated ore were reduced because of the presence of amorphous silica, defective silicates, and low crystallinity (Figure 2b).

### 3.2.5. Acid Consumption Analysis

Acid consumption is a major economic factor in the extraction of metal from their ores via heap leaching [42]. Therefore, different  $\text{H}_2\text{SO}_4$  concentrations and ore particulate sizes were tested for copper extraction to investigate  $\text{H}_2\text{SO}_4$  consumption in the heap leaching process (Figure 8). The amounts of  $\text{H}_2\text{SO}_4$  consumed (g of  $\text{H}_2\text{SO}_4$ /kg ore) during copper leaching at different pH values were calculated;  $\text{H}_2\text{SO}_4$  used for pH adjustment was also included. The copper extraction rate improved with a rise in acid concentration. A steep slope indicates a higher amount of acid consumption as compared to copper extraction, causing an economic loss (Figure 8). The copper extraction with 0.5 M  $\text{H}_2\text{SO}_4$  was approximately 72.4%, with 23.0 g of  $\text{H}_2\text{SO}_4$  consumption per kilogram of ore (Figure 6c). To approach a 73.0% extraction rate, acid consumption reached 28.8 g of  $\text{H}_2\text{SO}_4$  per kg of the ore sample. The amount of acid consumption to improve the copper extraction was up to 66.8%, which increased linearly; this was followed by an exponential rise caused by the minerals' dissolution and a subsequent release of metal ions (Figure 7). Protons ( $\text{H}^+$ ) played an important role in the chemical reactions of mineral dissolution (Table 3). Biotite and chlorite consumed 10 and 16 protons, respectively, for dissolution; thus, denoting their role as key acid consumers [35,38,43]. In this study, iron-rich chlorite and biotite were dominant in the ore samples. The solubility of both minerals in acid was relatively high. Thus, the continuous increase in Fe, Mg, and Al contents in the solution indicated that biotite and chlorite continuously dissolved during the study time, which resulted in acid consumption in the long term.

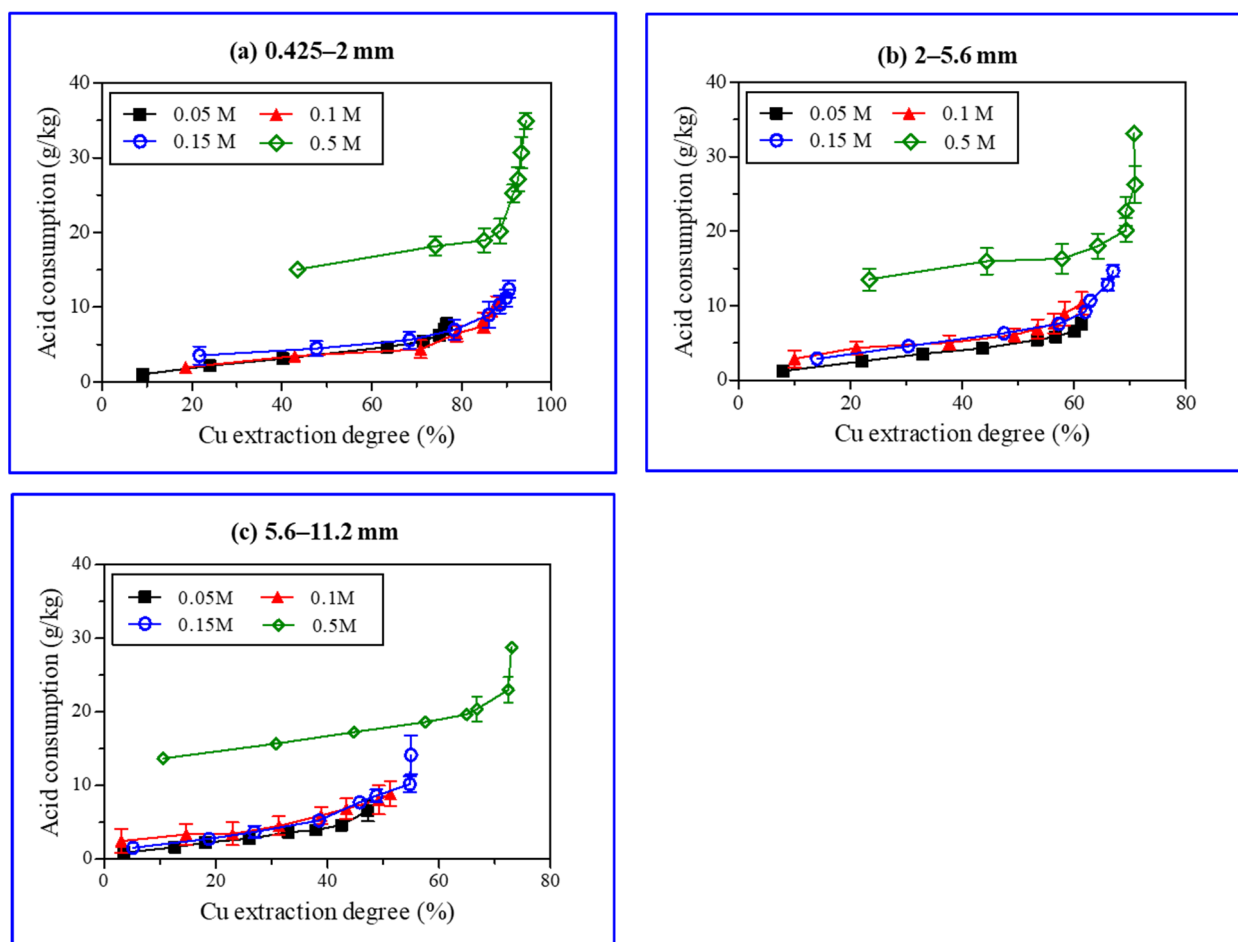


**Figure 8.** Sulfuric acid ( $H_2SO_4$ ) consumption (g/Kg) and copper extraction degree (%) during batch leaching experiments (0.425–2 mm (a), 2–5.6 mm (b), 5.6–11.2 mm (c)).

When the  $H_2SO_4$  concentration was high (0.5 M), acid consumption was higher (green, the diamond in Figure 8) than the copper extraction for the dissolution of gangue minerals. Hence, it is recommended to use a low  $H_2SO_4$  concentration. In general, the copper extraction rate for ore samples with particle sizes in the range of 5.6–11.2 mm and acid concentrations of 0.05–0.15 M of  $H_2SO_4$  was approximately 47–55%. However, in actual heap leaching, issues such as poor permeability and increased comminution costs will arise if an ore must be processed into smaller particles. Therefore, the ores should be crushed to achieve the particle size below 25 mm [10]. Thus, the pattern as depicted in Figure 8c may be observed in the case of a real heap leaching process. An increase in the particle size and low acid concentration suppresses copper extraction, rendering the leaching process as time consuming in achieving the desired copper extraction.

#### 4. Conclusions

The oxide ore in the Almalyk mine heap site (Uzbekistan) contained copper in an average grade of 1.56 wt% as malachite. Its major gangue minerals were quartz, orthoclase, muscovite, and chlorite. A weeklong (7 days) leaching experiment in batch mode indicated that the copper extraction rate was high with a smaller size of ore particles (0.425–2 mm) and a higher concentration of sulfuric acid ( $H_2SO_4$ ) (0.5 M). The copper extraction from relatively coarse particles (generally used in practical cases of heap leaching) decreased significantly with a slow reaction. During leaching, the dissolution of minerals in ore caused an increase in the content of copper and other metal ions in a PLS. The contents of Fe, Al, and Mg increased linearly with time because of the dissolution of relatively easy-to-dissolve silicate minerals (biotite and chlorite). The Cu and Ca showed a rapid increase in

the dissolution rate initially, followed by a gradual decrease caused by the dissolution of carbonate minerals (malachite and calcite). The acid consumption in comparison to copper extraction increased at the lag of the leaching experiment. The extra acid consumption was caused by the dissolution of gangue minerals (biotite and chlorite). Thus, in the case of actual heap leaching, the optimal leaching conditions should be determined by considering the factors such as acid consumption, extraction, and leaching time for cost-effective copper extraction.

**Author Contributions:** Data curation, S.-E.J.; writing—original draft preparation, C.-U.K., K.-W.C. and S.-E.J.; writing—review and editing, T.P., M.A.K., R.K., P.K. and Y.H.; project administration, D.-H.K.; funding acquisition, M.A.K. and B.-H.J. All authors have read and agreed to the published version of the manuscript.

**Funding:** This study was financially supported by the Korea Institute of Energy Technology Evaluation and Planning (KETEP) (No. 20182510102420) and Korea Environmental Industry & Technology Institute (KEITI) (No. 2020002480007). Moonis Ali Khan acknowledges the financial support through Researchers Supporting Project number (RSP-2021/345), King Saud University, Riyadh, Saudi Arabia.

**Data Availability Statement:** Not applicable.

**Conflicts of Interest:** The authors declare no conflict of interest.

## References

- Habbache, N.; Alane, N.; Djerad, S.; Tifouti, L. Leaching of copper oxide with different acid solutions. *Chem. Eng. J.* **2009**, *152*, 503–508. [[CrossRef](#)]
- Han, B.; Altansukh, B.; Haga, K.; Takasaki, Y.; Shibayama, A. Copper Recovery from Silicate-Containing Low-Grade Copper Ore Using Flotation Followed by High-Pressure Oxidative Leaching. *Resour. Process.* **2017**, *64*, 3–14. [[CrossRef](#)]
- Davenport, W.G.; King, M.J.; Schlesinger, M.E.; Biswas, A.K. *Extractive Metallurgy of Copper*, 4th ed.; Elsevier: Amsterdam, The Netherlands, 2002.
- Baba, A.A.; Ayinla, K.I.; Adekola, F.A.; Ghosh, M.K.; Ayanda, O.S.; Bale, R.B.; Sheik, A.R.; Pradhan, S.R. A review on novel techniques for chalcopyrite ore processing. *Int. J. Min. Eng. Miner. Process.* **2012**, *1*, 1–16. [[CrossRef](#)]
- Ata, O.N.; Çolak, S.; Ekin, Z.; Çopur, M. Determination of the optimum conditions for leaching of malachite ore in H<sub>2</sub>SO<sub>4</sub> solutions. *Chem. Eng. Technol.* **2001**, *24*, 409–413. [[CrossRef](#)]
- Bingöl, D.; Canbazoglu, M. Dissolution kinetics of malachite in sulphuric acid. *Hydrometallurgy* **2004**, *72*, 159–165. [[CrossRef](#)]
- Shabani, M.A.; Irannajad, M.; Azadmehr, A.R. Investigation on leaching of malachite by citric acid. *Int. J. Miner. Met. Mater.* **2012**, *19*, 782–786. [[CrossRef](#)]
- Panda, S.; Mishra, G.; Sarangi, C.K.; Sanjay, K.; Subbaiah, T.; Das, S.K.; Sarangi, K.; Ghosh, M.K.; Pradhan, N.; Mishra, B.K. Reactor and column leaching studies for extraction of copper from two low grade resources: A comparative study. *Hydrometallurgy* **2016**, *165*, 111–117. [[CrossRef](#)]
- Deng, J.; Wen, S.; Yin, Q.; Wu, D.; Sun, Q. Leaching of malachite using 5-sulfosalicylic acid. *J. Taiwan Inst. Chem. Eng.* **2017**, *71*, 20–27. [[CrossRef](#)]
- Petersen, J. Heap leaching as a key technology for recovery of values from low-grade ores—A brief overview. *Hydrometallurgy* **2016**, *165*, 206–212. [[CrossRef](#)]
- Bogdanović, G.D.; Stanković, V.D.; Trumić, M.S.; Antić, D.V.; Trumić, M.Ž. Leaching of low-grade copper ores: A case study for 'Kraku Bugaresku-Cementacija' deposits (Eastern Serbia). *J. Min. Met. A Min.* **2016**, *52*, 45–56. [[CrossRef](#)]
- Wu, A.; Yin, S.; Qin, W.; Liu, J.; Qiu, G. The effect of preferential flow on extraction and surface morphology of copper sulphides during heap leaching. *Hydrometallurgy* **2009**, *95*, 76–81. [[CrossRef](#)]
- Watling, H. The bioleaching of sulphide minerals with emphasis on copper sulphides—A review. *Hydrometallurgy* **2006**, *84*, 81–108. [[CrossRef](#)]
- Shayestehfar, M.; Nasab, S.K.; Mohammadalizadeh, H. Mineralogy, petrology, and chemistry studies to evaluate oxide copper ores for heap leaching in Sarcheshmeh copper mine, Kerman, Iran. *J. Hazard. Mater.* **2008**, *154*, 602–612. [[CrossRef](#)]
- Liu, M.; Wen, J.; Tan, G.; Liu, G.; Wu, B. Experimental studies and pilot plant tests for acid leaching of low-grade copper oxide ores at the Tuwu Copper Mine. *Hydrometallurgy* **2016**, *165*, 227–232. [[CrossRef](#)]
- Nicol, M.J. The kinetics of the dissolution of malachite in acid solutions. *Hydrometallurgy* **2018**, *177*, 214–217. [[CrossRef](#)]
- Hsu, P.-C.; Murr, L.E. A simple kinetic model for sulfuric acid leaching of copper from chrysocolla. *Met. Mater. Trans. A* **1975**, *6*, 435–440. [[CrossRef](#)]
- Nicol, M.; Akilan, C. The kinetics of the dissolution of chrysocolla in acid solutions. *Hydrometallurgy* **2018**, *178*, 7–11. [[CrossRef](#)]
- Bai, S.; Fu, X.; Li, C.; Wen, S. Process improvement and kinetic study on copper leaching from low-grade cuprite ores. *Physicochem. Probl. Miner. Process.* **2018**, *54*, 300–310.
- Quast, K. Leaching of atacamite (Cu<sub>2</sub>(OH)<sub>3</sub>Cl) using dilute sulphuric acid. *Miner. Eng.* **2000**, *13*, 1647–1652. [[CrossRef](#)]

21. Helle, S.; Kelm, U. Experimental leaching of atacamite, chrysocolla and malachite: Relationship between copper retention and cation exchange capacity. *Hydrometallurgy* **2005**, *78*, 180–186. [[CrossRef](#)]
22. Golovanov, I.M.; Seltmann, R.; Kremenetsky, A.A. The porphyry Cu–Au/Mo deposits of Central Euroasia: 2. The Almalyk (Kalmakyr–Dalnee) and Saukbulak Cu–Au porphyra systems, Uzbekistan. In *Super Porphyry Copper and Gold Deposits: A Global Perspective*; Poter, T.M., Ed.; PGC Publishing: Adelaide, Australia, 2005; pp. 513–523.
23. Shukurov, N.; Kodirov, O.; Peitzsch, M.; Kersten, M.; Pen-Mouratov, S.; Steinberger, Y. Coupling geochemical, mineralogical and microbiological approaches to assess the health of contaminated soil around the Almalyk mining and smelter complex, Uzbekistan. *Sci. Total Environ.* **2014**, *476*, 447–459. [[CrossRef](#)] [[PubMed](#)]
24. Sillitoe, R.H. Andean copper province: Tectonomagmatic settings, deposit types, metallogeny, exploration, and discovery. *Econ. Geol. 100th Anniv. Vol.* **2005**, 845–890.
25. Cheng, Z.; Zhang, Z.; Chai, F.; Hou, T.; Santosh, M.; Turesebekov, A.; Nurtaev, B.S. Carboniferous porphyry Cu–Au deposits in the Almalyk orefield, Uzbekistan: The Sarycheku and Kalmakyr examples. *Int. Geol. Rev.* **2018**, *60*, 1–20. [[CrossRef](#)]
26. Xue, C.J.; Zhao, X.B.; Mo, X.X.; Chen, Y.C.; Dong, L.H.; Gu, X.X.; Zhang, Z.C.; Nurtaev, B.; Pak, N.; Li, Z.D.; et al. Tectonic-metallogenic evolution of Western Tianshan giant Au–Cu–Zn–Pb metallogenic belt and prospecting orientation. *Acta Geol. Sin.* **2014**, *88*, 2490–2531.
27. Dill, H.G. The “chessboard” classification scheme of mineral deposits: Mineralogy and geology from aluminum to zirconium. *Earth-Sci. Rev.* **2010**, *100*, 1–420. [[CrossRef](#)]
28. Chen, M.; Ma, L.Q. Comparison of Three Aqua Regia Digestion Methods for Twenty Florida Soils. *Soil Sci. Soc. Am. J.* **2001**, *65*, 491–499. [[CrossRef](#)]
29. Berger, B.R.; Ayuso, R.A.; Wynn, J.C.; Seal, R.R. *Preliminary Model of Porphyry Copper Deposits*; U.S. Geological Survey: Washington, DC, USA, 2008; Volume 1321, p. 55. [[CrossRef](#)]
30. Gettens, R.J.; Fitzhugh, E.W. Malachite and green verditer. *Stud. Conserv.* **1974**, *19*, 2–23.
31. Levenspiel, O. Chemical reaction engineering. *Ind. Eng. Chem. Res.* **1999**, *38*, 4140–4143. [[CrossRef](#)]
32. Sun, X.-L.; Chen, B.-Z.; Yang, X.-Y.; Liu, Y.-Y. Technological conditions and kinetics of leaching copper from complex copper oxide ore. *J. Cent. South Univ. Technol.* **2009**, *16*, 936–941. [[CrossRef](#)]
33. Kokes, H.; Morcali, M.; Acma, E. Dissolution of copper and iron from malachite ore and precipitation of copper sulfate pentahydrate by chemical process. *Eng. Sci. Technol. Int. J.* **2014**, *17*, 39–44. [[CrossRef](#)]
34. Deshenthree, C. Acid-gangue interactions in heap leach operations: A review of the role of mineralogy for predicting ore behaviour. *Minerals* **2018**, *8*, 47.
35. Jansen, M.; Taylor, A. Overview of gangue mineralogy issues in oxide copper heap leaching. In Proceedings of the ALTA Conference, Perth, Australia, 6–9 July 2003.
36. Alkattan, M.; Oelkers, E.H.; Dandurand, J.L.; Schott, J. An experimental study of calcite and limestone dissolution rates as a function of pH from –1 to 3 and temperature from 25 to 80 °C. *Chem. Geol.* **1998**, *151*, 199–214. [[CrossRef](#)]
37. Seyedbagheri, A.; McLaren, C.; Van Staden, P. *A Study of Acid-Gangue Reactions in Heap Leach Operations*; Mintek: Randburg, South Africa, 2009.
38. Youlton, B.; Kinnaird, J. Gangue–reagent interactions during acid leaching of uranium. *Miner. Eng.* **2013**, *52*, 62–73. [[CrossRef](#)]
39. Terry, B. The acid decomposition of silicate minerals part I. Reactivities and modes of dissolution of silicates. *Hydrometallurgy* **1983**, *10*, 135–150. [[CrossRef](#)]
40. Apostolidis, C.; Distin, P. The kinetics of the sulphuric acid leaching of nickel and magnesium from reduction roasted serpentine. *Hydrometallurgy* **1978**, *3*, 181–196. [[CrossRef](#)]
41. Kothukov, S.V.; Giganov, G.P.; Karimov, E.V.; Sologub, D.V. Tests of a combined technology for the treatment of mixed copper-containing concentrates. *Tsvetnye Met.* **1988**, *1*, 20–22.
42. Rich, R. *Inorganic Reactions in Water*, 1st ed.; Springer: Berlin, Germany, 2007.
43. Free, M.L. Understanding Acid Consumption and Its Relationship with Copper Recovery. In Proceedings of the SME Annual Meeting and Exhibit 2010, Phoenix, AZ, USA, 28 February–3 March 2010.